Local Buckling of Steel Plates in Double Skin Composite Panels under Biaxial Compression and Shear

Qing Quan Liang, MASCE[1]; Brian Uy, M.ASCE[2]; Howard D. Wright[3]; and Mark A. Bradford, M.ASCE[4]

Abstract: Steel plates in double skin composite (DSC) panels are restrained by a concrete core and welded stud shear connectors at discrete positions. Local buckling of steel plates in DSC panels may occur in a unilateral mode between stud shear connectors when subjected to combined states of stresses. This paper studies the local and post-local buckling strength of steel plates in DSC panels under biaxial compression and in-plane shear by using the finite element method. Critical local buckling interaction relationships are presented for steel plates with various boundary conditions that include the shear stiffness effects of stud shear connectors. A geometric and material nonlinear analysis is employed to investigate the post-local buckling interaction strength of steel plates in biaxial compression and shear. The initial imperfections of steel plates, material yielding and the nonlinear shear-slip behavior of stud shear connectors are considered in the nonlinear analysis. Design models for critical buckling and ultimate strength interactions are proposed for determining the maximum stud spacing and ultimate strength of steel plates in DSC panels.

CE Database keywords: Biaxial stress; Buckling; Composite structures; Finite element method; Postbuckling; Shear; Strength.

---

[1] Research Fellow, School of Civil and Environmental Engineering, The University of New South Wales, Sydney, NSW 2052, Australia. E-mail: stephenl@civeng.unsw.edu.au
[2] Associate Professor, School of Civil and Environmental Engineering, The University of New South Wales, Sydney, NSW 2052, Australia.
[3] Professor, Department of Civil Engineering, University of Strathclyde, Glasgow, G4 0NG, United Kingdom.
[4] Professor, School of Civil and Environmental Engineering, The University of New South Wales, Sydney, NSW 2052, Australia.

Introduction

Double skin composite (DSC) panels are innovative and efficient structural systems that can be used in submerged tube tunnels (Tomlinson et al. 1989), nuclear structures, liquid and gas containment structures, military shelters, offshore structures, bridges and shearwalls in buildings. A DSC panel is formed by placing concrete between two steel plates welded with headed stud shear connectors at a regular spacing, as illustrated in Fig. 1. Stud shear connectors are used to resist shear between steel plates and the concrete core as well as separation at the interface. Steel plates serve as biaxial steel reinforcement and permanent formwork for the concrete core. When DSC panels are used as slabs or shearwalls, the steel plates may be subjected to biaxial compression and in-plane shear. In DSC panels, local buckling of steel plates in combined states of stresses may occur between shear connectors, depending on the stud spacing and plate thickness.

Considerable research effort has been made to investigate the behavior and design of DSC elements. Oduyemi and Wright (1989) and Wright et al. (1991a) have conducted experiments on DSC elements. Experimental and theoretical studies showed that DSC elements could be analyzed and designed in accordance with conventional theories for doubly reinforced concrete elements and composite structures, providing that the effects of local buckling and shear connection failures are adequately taken into consideration (Wright et al. 1991b; Wright and Oduyemi 1991). Tests and analysis of DSC beams carried out by Roberts et al. (1996) showed that DSC beams failed by the yielding of the tension plate when the stud spacing to compressed plate thickness ratio was limited to 40. Shanmugam et al. (2002) also studied the load-deformation behavior of DSC slabs by using the finite element modeling technique.

Thin steel plates in contact with concrete are constrained to buckle locally in one lateral direction when subjected to compression. The importance of understanding this unilateral stability problem has been highlighted in recent published work. Ge and Usami (1992, 1994) conducted tests and numerical analysis on the local buckling of concrete-filled steel box columns with and without internal stiffeners. Limiting width-to-thickness ratios derived by Wright (1993, 1995) are useful for proportioning steel plates under uniaxial compression and shear. Experimental and theoretical research into the behavior and design of composite members including local buckling effects has been undertaken by Uy and Bradford (1995), Bridge et al. (1995), Uy (2000) and Uy et al. (2001). In addition, Liang and Uy (1998, 2000) incorporated their effective width models into the ultimate strength design of concrete-filled steel box columns. Moreover, Bradford et al. (2000) presented slenderness limits for steel plates bolted to the sides of reinforced concrete beams. The local and post-local buckling interaction strength of steel plates under combined biaxial compression and shear in DSC panels, however, has not been reported in the literature.

The strength of steel plates in biaxial compression has been studied by using various methods. Williams and Walker (1975) used the perturbation method to investigate the post-buckling behavior of biaxially loaded plates incorporating geometric imperfections and residual stresses. Little (1977) presented an energy method for the collapse analysis of steel plates with geometric imperfections under in-plane biaxial compression. Nonlinear finite element analysis was utilized by Valsgard (1980) to predict the biaxial strength of steel plates in ship structures. This study suggested that the biaxial strength should be determined on the basis of the proportional load increment approach in a nonlinear analysis. Dier and Dowling (1984) employed a finite difference approach to investigate the strength interaction relationships of plates subjected to biaxial forces that included compression and tension. Moreover, tests on

steel plates under biaxial compression have been undertaken by Bradfield et al. (1992). Guedes Soares and Gordo (1996) presented a survey of existing equations for the ultimate strength assessment of steel plates under biaxial loads.

The biaxial compressive and in-plane shear stresses may coexist in plated structures, such as ship structures, slabs and shearwalls. Shear can have a significant effect on the strength performance of these structural elements. Davidson et al. (1989) used the ultimate strength of steel plates under uniaxial compression obtained by elasto-plastic analysis in analytical models to determine the interaction strength of steel plates subjected to shear and biaxial compression. Mendera (1994) presented interaction stability criteria for steel plates and shells in combined states of stresses. The buckling and ultimate strength interaction relationships for flat plates under in-plane biaxial and shear forces were studied by Ueda et al. (1995). These studies employed the von Mises yield criterion to express the strength interaction relationship for stocky plates.

The local and post-local buckling behavior of steel plates in DSC panels under biaxial compression has been investigated by Liang et al. (2003). This paper extends the previously cited work to include the effects of in-plane shear stresses on the local and post-local buckling strength of steel plates in DSC panels. Finite element models, which account for initial imperfections, material stress-strain laws and the shear-slip behavior of headed stud shear connectors, are described. Numerical results for the critical buckling interactions of steel plates with various boundary conditions and for the ultimate strength interactions of steel plates with various width-to-thickness ratios are presented and discussed. Design models for buckling and strength interactions are proposed for the design of steel plates in DSC panels subjected to biaxial compression and shear, and are compared with existing results.

Finite Element Analysis

General

In the present study, the finite element code STRAND7 (2000) was utilized to investigate the critical local and post-local buckling strength of steel plates in DSC panels under biaxial compression and shear. Linear buckling analysis based on the bifurcation buckling theory was undertaken to predict the critical buckling interaction relationships of perfectly flat steel plates. The post-local buckling strength interactions of steel plates with initial imperfections were investigated by performing a geometric and material nonlinear analysis. The plasticity of a steel plate was treated using the von Mises yield criterion in the nonlinear analysis, in which the plate was divided into ten layers through its thickness. An eight-node quadrilateral plate/shell element was employed in all analyses. A 20 × 20 mesh was used to discretize a plate in the linear buckling analysis. A 10 × 10 mesh was employed in the nonlinear analysis and was found to be economic and adequate to yield accurate results for use in practice.

Boundary Conditions

In DSC panels, steel plates are restricted to buckle locally between stud shear connectors when subjected to combined states of stresses. To simulate this buckling situation, the structural model was considered to be a single plate field between stud shear connectors, as shown in Fig. 2. This model visualization enables the maximum stud spacing to plate thickness ratio and the ultimate strength of a single plate field to be determined (Liang et al. 2003). The edge restraint depends on the stiffness of adjacent plate fields. It could be argued that the edges of the plate field are restrained from rotation by the adjacent plate fields and

concrete, but the degree of restraint is not complete as adjacent plate fields in a DSC panel are usually not stiff enough to offer a fully clamped boundary condition. It was assumed that the edges of the plate field between stud shear connectors at a worst case were hinged. This means that the edges of the plate field between stud shear connectors can rotate unilaterally but cannot deflect out of the plane. The plate field is welded with stud shear connectors of finite shear stiffness at its corners. Therefore, rotations at the corners are not permitted and their in-plane translations can be defined by the shear-slip model. This situation is similar to the simply supported boundary condition with additional restraint offered by shear connectors, and is denoted as S-S-S-S+SC (S = simply supported; SC = shear connectors). In actual construction, DSC panels as slabs and walls are used to build up a structure. The boundaries of a DSC panel are connected with reinforced concrete elements that rotationally restrain the boundaries of the panel. Therefore, the edge of a plate field located at the boundary of a DSC panel could be assumed as clamped. The boundary condition assumed for plate fields in DSC panels provided a good correlation with experimental results (Liang et al. 2003).

Initial Imperfections

The initial imperfections of steel plates are present in the form of initial out-of-plane deflections and residual stresses. Initial imperfections cause reductions in the strength and stiffness of steel plates and are thus considered in the post-local buckling analysis. Different magnitudes of geometric imperfections have been used in the nonlinear analysis of steel plates (Williams and Walker 1975; Valsgard 1980; Dier and Dowling 1984; Davidson et al. 1989). The effect of initial geometric imperfections on the post-local buckling strength of steel plates in contact with concrete has been investigated by Liang and Uy (2000). In the present study,

the form of initial deflections was taken as the first local buckling mode under biaxial compression due to the fact that it is unlikely in practice to be dominated by the critical shear-buckling mode (Davidson et al. 1989; Liang and Uy 2000; Liang et al. 2003). The maximum magnitude of initial geometric imperfections at the plate centre was taken as $w_0 = 0.003b$ for steel plates in DSC panels, as suggested by Wright (1993). A lateral pressure was applied to the plate to induce the initial geometric imperfections (Liang and Uy 2000). Residual stresses due to welding of stud shear connectors at discrete positions are less critical in DSC panels compared to continuously welded plate structures. Their effects were not considered in the model.

Stress-Strain Relationship for Steel Plates

The formula proposed by Ramberg and Osgood (1943) was employed in the nonlinear finite element analysis to define the material stress-strain relationship for steel plates. The formula is expressed by

$$\varepsilon = \frac{\sigma}{E}\left[1 + \frac{3}{7}\left(\frac{\sigma}{\sigma_{0.7}}\right)^n\right] \tag{1}$$

where σ = stress; ε = strain; E = the Young's modulus; $\sigma_{0.7}$ = the stress corresponding to $E_{0.7} = 0.7E$; and n = the knee factor that defines the sharpness of the knee in the stress-strain curve. The knee factor n = 25 was adopted in the present study to account for the isotropic strain hardening of steel plates (Mofflin and Dwight 1984; Liang and Uy 2000). The stress $\sigma_{0.7}$ can be determined from the experimental stress-strain curve of steel plates. Since the proof-yield stress and strain of structural steel are usually known, $\sigma_{0.7}$ can also be calculated

by substituting them into Eq. (1). An ultimate strain of 0.25 was applied to mild steel in the nonlinear analysis.

Shear-Slip Relationship for Stud Shear Connectors

Shear connectors influence the stability performance of steel plates in DSC panels. Stud shear connectors with finite shear stiffness enhance the resistance of simply supported steel plates to local buckling. Slender steel plates in DSC panels may buckle locally before shearing failure of stud shear connectors. On the other hand, stud shear connectors may fracture before stocky steel plates attain the full plastic capacities. In addition, interaction modes between local buckling and shear connection failure may exist. Therefore, the behavior of shear connectors must be considered in both the linear buckling and nonlinear analyses in order to give realistic design guidelines.

The behavior of shear connectors in composite construction is expressed by the shear-slip relationship, which can be determined by push-out tests (Ollgaard et al. 1971; Oehlers and Coughlan 1986; Liang and Patrick 2001). The shear-slip model for stud shear connectors proposed by Ollgaard et al. (1971) was adopted in the present study, and it is expressed by

$$Q = Q_{\mathrm{u}}\left(1 - e^{-18\delta}\right)^{0.4} \tag{2}$$

where Q = the longitudinal shear force (N); Q_{u} = the ultimate shear strength of a stud shear connector (N); and δ = the longitudinal slip (mm). In AS 2327.1 (1996), the ultimate shear strength of a stud shear connector is calculated as the lesser value from the following equations:

$$Q_u = 0.63 d_{bs}^2 f_{uc} \tag{3a}$$

$$Q_u = 0.31 d_{bs}^2 \sqrt{f_{cj}^{'} E_c} \tag{3b}$$

where d_{bs} = the shank diameter of a headed stud connector (mm); f_{uc} = the material characteristic tensile strength of shear connectors (MPa); $f_{cj}^{'}$ = the characteristic compressive strength of concrete after j days caring (MPa); and E_c = the elastic modulus of concrete (MPa). It should be noted that Eq. (2) was derived from the results of push-out tests in which the specimens were constructed by concrete slabs attached to steel beams. A DSC panel would offer greater confinement to the concrete than a composite beam. This beneficial effect was not considered in the present study.

If 19-mm diameter headed stud shear connectors (f_{uc} = 410 MPa) are used in a DSC panel filled with concrete of a characteristic compressive strength of 32 MPa, Eq. (3) yields an ultimate shear strength of 93 kN. A shear-slip curve for 19-mm diameter headed stud shear connectors obtained by using Eq. (2) is shown in Fig. 3. In the linear buckling analysis, a stud shear connector was modeled by using linear spring elements. The spring stiffness was taken as the tangent modulus of the shear-slip curve. In the post-local buckling analysis, a spring-type beam element was employed to model stud shear connectors whose nonlinear shear-slip relationship was defined by Eq. (2).

Numerical Results for Buckling Interaction

General

The linear buckling analysis allows for the critical combinations of buckling stresses for steel plates under combined biaxial compression and shear to be determined. After the buckling analysis, the elastic buckling coefficients can be calculated from the following well-known equations (Bulson 1970):

$$\sigma_{xcr} = \frac{k_x \pi^2 E}{12(1-\nu^2)(b/t)^2} \tag{4}$$

$$\sigma_{ycr} = \frac{k_y \pi^2 E}{12(1-\nu^2)(a/t)^2} \tag{5}$$

$$\tau_{xycr} = \frac{k_{xy} \pi^2 E}{12(1-\nu^2)(b/t)^2} \tag{6}$$

where a = the length of a plate field; b = the width of a plate field; σ_{xcr} = the critical buckling stress in the x direction; σ_{ycr} = the critical buckling stress in the y direction; τ_{xycr} = the critical shear buckling stress; k_x = the elastic buckling coefficient in the x direction; k_y = the elastic buckling coefficient in the y direction; k_{xy} = the elastic shear buckling coefficient; ν = Poisson's ratio; and t = the thickness of the plate.

Under a single stress component, the buckling coefficient is used to account for the effects of the plate aspect ratio and boundary condition on the critical buckling stress. In combined states of stresses, the buckling coefficient also needs to account for the interaction effects of biaxial compression and shear on the critical buckling stress. Elastic buckling coefficients were obtained for square steel plates with three boundary conditions, which were S-S-S-S+SC, C-S-S-S+SC and C-C-S-S+SC (S = simply supported; C = clamped; SC = shear connectors). The configurations of plates used in all analyses were a = b = 500 mm, t = 10

mm, $E = 200$ GPa and $\nu = 0.3$. If a stud shear connector is at the boundary of a DSC panel and resists shear from a single plate field, the shear stiffness $k_s = 4.52 \times 10^6$ N/mm was used in the analysis. If a stud resists shear from two adjacent plate fields, the stud shear stiffness was taken as $0.5k_s$ regardless of its location. The applied stress ratios $\tau_{xy} / \sigma_x = 0.0$, 0.5, 1.0, 4/3, 2.0, 4.0, 5.0 and $\sigma_x / \tau_{xy} = 0$ were used in the buckling analysis to develop a complete interaction curve for plates.

Buckling Interaction Curves

Fig. 4 shows the critical local buckling interaction curves for steel plates with the S-S-S-S+SC boundary condition. It can be observed from Fig. 4 that the presence of shear stresses reduces the critical buckling strength of plates in both longitudinal and transverse directions. Increasing biaxial compressive stresses reduces the critical shear buckling strength of a plate. Fig. 4 also demonstrates the effects of the ratio of transverse to longitudinal loading ($\alpha = \sigma_y / \sigma_x$) on buckling interaction relationships for plates in combined states of stresses. It is seen that the presence of transverse loading (σ_y) significantly reduces the longitudinal critical buckling stress and considerably reduces the critical shear buckling stress. When no shear stresses are applied to the plate, the effect of transverse loading on the critical buckling strength of the plate in the *x* direction is most pronounced. This effect is reduced due to the interaction of compression and shear. The buckling coefficient for pure shear is 10.84. The interaction between k_x and k_y in the presence of shear stresses with a constant value of τ_{xy} / τ_{xycr} is given in Fig. 5. These buckling interaction curves are linear because steel plates buckle in a single half-wave mode.

Buckling interaction curves for square plates with the boundary condition of C-S-S-S+SC are presented in Fig. 6. It is seen that the elastic buckling coefficient for plates under pure shear is 14.25. When the biaxial loading ratio α is increased from zero to 0.25, 0.5, 1.0 and 1.5, the elastic buckling coefficient for plates under biaxial compression is reduced from 5.55 to 4.71, 4.06, 3.17 and 2.59, respectively. Fig. 7 shows the buckling interaction curves for plates with two adjacent edges clamped (C-C-S-S+SC). It can be observed from Fig. 7 that the elastic buckling coefficient for plates in pure shear is 18.6. When α increases from zero to 0.25, 0.5, 1.0 and 1.5, the buckling coefficient for plates in biaxial compression decreases from 7.8 to 6.56, 5.51, 4.22 and 3.36, respectively. It is evident that the clamped edges considerably increase the stability performance of steel plates under combined biaxial compression and shear.

Numerical Results for Strength Interaction

General

The post-local buckling interaction strength of steel plates with the boundary condition of S-S-S-S+SC was investigated here. For a plate with a specific aspect ratio, slenderness and initial imperfection, the ultimate strength depends on the biaxial compression and shear forces. A strength interaction curve for a plate was developed by varying the applied shear and normal stresses in the nonlinear analysis. The applied stress ratios τ_{xy}/σ_x = 0.0, 0.2, 0.4, 0.6, 1.0, 2.0, 2.5, 5.0 and σ_x/τ_{xy} = 0 were used in the analysis. This study employed the proportional load increment scheme, in which the ratio of applied shear stress to biaxial compressive stress was kept constant at each load increment in a nonlinear analysis. Square steel plates (400 × 400 mm) with a yield stress of σ_0 = 300 MPa subjected to shear and equal

biaxial compressive stresses ($\alpha = 1$) were studied. The 19-mm diameter headed studs were used as shear connectors in the DSC panel filled with concrete having a compressive strength of 32 MPa. Half of the ultimate shear strength of a stud shear connector was used in Eq. (1) to account for the effect of the adjacent plate field.

Strength Interaction Curves

The strength interaction curves for square steel plates with various *b/t* ratios obtained from the results of a nonlinear finite element analysis are shown in Fig. 8. These curves were normalized to the yield stress of steel plates. The shear yield stress τ_0 was taken as $\sigma_0 / \sqrt{3}$. It can be observed that the ultimate strength of a plate under the combined states of stresses generally decreases with an increase in the *b/t* ratio. The ultimate strength of steel plates in two directions is reduced by the presence of shear stresses. Due to the effects of local buckling, shear connection failure and initial imperfections, steel plates under biaxial compression only cannot attain the yield strength, as shown in Fig. 8. The ultimate strength of the stocky plate with a *b/t* ratio of 20 under pure shear is less than the shear yield stress because of the shearing failure of the stud shear connectors. In contrast, the strength of a slender plate a the *b/t* ratio of 100 is governed by elastic local buckling. It should also be noted that the ultimate strength of steel plates in the *x* direction is greatly reduced by any significant transverse loading.

Proposed Design Models

Design Models for Buckling Interaction

It can be observed from Figs. (4), (6) and (7) that the shapes of buckling interaction curves for plates with a specific aspect ratio and boundary condition vary with biaxial loads. By normalizing these interaction curves to the buckling coefficients of plates under a single stress component such as shear stress alone or biaxial compressive stress, it was found that the shapes of the curves were identical for the same boundary condition. Fig. 9 shows the normalized buckling interaction curves for plates with various boundary conditions. To express these curves, design models for critical buckling interactions of square plates under biaxial compression and shear are proposed as

$$\left(\frac{k_{\mathrm{x}}}{k_{\mathrm{xo}}}\right)^{\xi}+\left(\frac{k_{\mathrm{xy}}}{k_{\mathrm{xyo}}}\right)^{2}=1 \tag{7}$$

where k_{xo} = the buckling coefficient in the x direction in the absence of shear stresses; k_{xyo} = the shear buckling coefficient in the absence of biaxial compression; and ξ = the buckling shape factor that defines the shape of a buckling interaction curve. The values of buckling coefficients k_{xo} and k_{xyo} for steel plates with different boundary conditions are given in Table 1 for design. The buckling shape factors proposed in Table 1 are shown to be adequate to express the buckling interaction curves of plates with these boundary conditions. It is seen from Table 1 that the buckling shape factor increases with an increase in the restraints of the plate edges. Eq. (7) is also applicable to the interaction of k_{y} and k_{xy}.

Buckling coefficients presented can be used to determine the limiting width-to-thickness ratios for steel plates under biaxial compression and shear in DSC panels. This ensures that the elastic local buckling of steel plates between stud shear connectors will not occur before

steel yielding. The relationship between critical buckling stress components at yield can be expressed by the von Mises yield criterion as

$$\sigma_{\mathrm{xcr}}^2 - \sigma_{\mathrm{xcr}}\sigma_{\mathrm{ycr}} + \sigma_{\mathrm{ycr}}^2 + 3\tau_{\mathrm{xycr}}^2 = \sigma_0^2 \tag{8}$$

If the material properties E = 200 GPa and ν = 0.3, and the plate aspect ratio $\varphi = a/b$ are used, the limiting width-to-thickness ratio can be derived by substituting Eqs. (4), (5) and (6) into Eq. (8) as

$$\frac{b}{t}\sqrt{\frac{\sigma_0}{250}} = 26.89\left(k_{\mathrm{x}}^2 - \frac{k_{\mathrm{x}}k_{\mathrm{y}}}{\varphi^2} + \frac{k_{\mathrm{y}}^2}{\varphi^4} + 3k_{\mathrm{xy}}^2\right)^{1/4} \tag{9}$$

An example is presented herein to illustrate the application of the proposed design models for determining the maximum stud spacing in DSC panels. Stresses acting at the edges of a plate field in a DSC panel can be determined by undertaking a global stress analysis on the DSC panel. If the spacing of stud shear connectors is the same in two directions, only square plate fields need to be considered. It is assumed that a plate field ($\varphi = 1$) with the S-S-S-S+SC boundary condition is subjected to biaxial compressive stresses ($\alpha = 1$) and shear stress $\tau_{\mathrm{xy}} = 0.5\sigma_{\mathrm{x}}$. This gives $k_{\mathrm{x}} = k_{\mathrm{y}}$ and $k_{\mathrm{xy}} = 0.5k_{\mathrm{x}}$ according to Eqs. (4-6). From Table 1, parameters for buckling interactions can be obtained as k_{xo} = 2.404, k_{xyo} = 10.84, and ξ = 1.1. By substituting these parameters into Eq. (7), buckling coefficients are obtained as $k_{\mathrm{x}} = 2.38$ and $k_{\mathrm{xy}} = 1.19$. By using Eq. (9), the limiting width-to-thickness ratio for this plate field with a yield stress of 250 MPa is 48. If the compression steel skin with a thickness of 10 mm is used, the maximum stud spacing in two directions in this DSC panel is 480 mm.

Design Models for Strength Interaction

It is seen from Fig. 8 that the shape of strength interaction curves strongly depends on the plate slenderness. If these strength interaction curves are normalized to the ultimate strength of plates subjected to either pure shear or biaxial compression, the form of Eq. (7) can be used to express them for plates under combined states of stresses. Design models for ultimate strength interactions are proposed as

$$\left(\frac{\sigma_{xu}}{\sigma_{xuo}}\right)^{\zeta}+\left(\frac{\tau_{xyu}}{\tau_{xyuo}}\right)^{2}=1 \tag{10}$$

where σ_{xu} = the ultimate strength of a plate in *x* direction under biaxial compression and shear; σ_{xuo} = the ultimate strength of a plate in *x* direction under biaxial compression only; τ_{xyu} = the ultimate shear strength of a plate ; τ_{xyuo} = the ultimate strength of a plate under pure shear only; and ζ = the strength shape factor of the ultimate strength interaction curve, which depends on the plate slenderness. The ultimate strength of square steel plates under either biaxial compression or shear alone is given in Table 2. Based on numerical results, the strength shape factors for plates with various slenderness ratios are proposed in Table 2. By using Eq. (10) and Table 2, the strength interaction curves for plates with various slenderness ratios are plotted in Fig. 10. It should be noted that the curves presented here are for plates subjected to the same normal stresses in both directions ($\alpha=1$).

A square plate field with a *b/t* ratio of 40 in a DSC panel under biaxial compression ($\alpha=1$) and shear is considered here to demonstrate the application of the proposed strength design models. The applied shear stress is equal to $0.6\sigma_x$. This gives $\tau_{xyu}=0.6\sigma_{xu}$. The yield stress

of the steel plate is 300 MPa and shear yield stress is $300/\sqrt{3}$ MPa. The parameters for strength interaction can be obtained from Table 2 as σ_{xuo}/σ_0 = 0.481, τ_{xyuo}/τ_0 = 1.0, and $\zeta = 1.6$. By substituting these known values into Eq. (10), the ultimate strength σ_{xu} can be determined as 127 MPa and the ultimate shear strength (τ_{xyu}) is 76.2 MPa. The only unknown in Eq. (10) can be easily solved using a spreadsheet.

Comparison with Existing Results

The proposed design models for the ultimate strength interactions of steel plates in combined biaxial compression and shear are compared with the results given by Davidson et al. (1989). Fig. 11 shows strength interaction curves for square steel plates with a *b/t* ratio of 40 and under biaxial compression ($\alpha = 1$) and shear. The interaction curve given by the present study was generated using Eq. (10) for a plate with the S-S-S-S+SC boundary condition in a DSC panel. The curve obtained by Davidson et al. was for a simply supported steel plate that was not restrained by shear connectors. For the case of Davidson et al., the ultimate strength of the square plate depended on the plate slenderness but not on its width. It is seen from Fig. 11 that the normalized ultimate strength interaction curve obtained by the proposed design model agrees well with that given by Davidson et al.

Conclusions

This paper has investigated the critical local buckling and ultimate strength of steel plates in double skin composite panels under combined biaxial compression and shear by using the finite element analysis method. The finite element models developed have incorporated initial imperfections, material stress-strain behavior and the shear-slip characteristics of stud shear

connectors. Critical buckling interaction relationships have been developed for steel plates with various boundary conditions. Strength interaction curves have been generated by using the proportional load increment method in the nonlinear analysis for square plates with various width-to-thickness ratios. Design models for critical buckling and ultimate strength interactions have also been proposed for the design of square plates in DSC panels under biaxial compression and shear.

The elastic buckling coefficients and design models for the buckling interactions of steel plates presented can be used to determine the critical stud spacing in DSC panels. This critical stud spacing predicted ensures that the critical local buckling of steel plates between stud shear connectors is prevented before the yielding of steel plates. Numerical investigations show that the ultimate strength of stocky plates is governed by the shear capacity of stud shear connections or local buckling of steel plates. Slender steel plates can attain their full post-local buckling reserve of strength without the premature fracture of stud shear connectors.

This paper has focused on square steel plate fields in combined states of stresses in DSC panels in which shear connectors were placed at the same spacing in two directions. The proposed design models can be used in practice for the design of DSC panels with similar design situations. The finite element models and interaction equations developed can be extended to other design situations in DSC construction. If the size of a square plate field is larger than that used in the present study, the strength design equation can still be used but the values of σ_{xuo} and τ_{xyuo} have to be determined. This is because of the limiting capacity of stud shear connectors. Experiments on the collapse behavior of DSC panels are needed to examine further the efficiency of proposed design models in evaluating the overall performance of DSC panels.

Notation

The following symbols are used in this paper:

a = length of plate field between shear connectors;

b = width of plate field between shear connectors;

d_{bs} = shank diameter of a headed stud;

E = Young's modulus of elasticity;

$E_{0.7}$ = secant modulus $E_{0.7} = 0.7E$;

E_{c} = elastic modulus of concrete;

f'_{cj} = characteristic compressive strength of concrete at the j days;

f_{uc} = material characteristic tensile strength of shear connector;

k_{s} = shear stiffness of shear connector;

k_{x} = elastic local buckling coefficient in the x direction;

k_{y} = elastic local buckling coefficient in the y direction;

n = knee factor of material stress-strain curve;

Q = longitudinal shear force;

Q_{u} = ultimate shear strength of shear connector;

t = thickness of steel plate;

w_0 = initial out-of-plane deflection;

α = ratio of transverse to longitudinal loading, $\alpha = \sigma_y / \sigma_x$;

δ = longitudinal slip;

ξ = buckling shape factor of buckling interaction curves;

ζ = strength shape factor of strength interaction curves;

ε = strain;

ν = Poisson's ratio;

σ = stress;

σ_0 = yield stress or 0.2% proof stress;

$\sigma_{0.7}$ = stress corresponding to $E_{0.7} = 0.7E$;

σ_x = applied edge stress in x direction;

σ_{xcr} = critical buckling stress in x direction;

σ_{xu} = ultimate strength of plate in x direction;

σ_{xuo} = ultimate strength of plate in x direction under biaxial compression only;

σ_y = applied edge stress in y direction;

σ_{ycr} = critical buckling stress in y direction;

τ_0 = shear yield stress;

τ_{xy} = applied shear stress;

τ_{xycr} = critical shear buckling stress;

τ_{xyu} = ultimate shear strength of plate;

τ_{xyuo} = ultimate shear strength of plate under pure shear;

φ = plate aspect ratio, $\varphi = a/b$.

References

AS 2327.1 (1996). *Composite Structures, Part I: Simply Supported Beams*. Standard Australia, Sydney.

Bradfield, C. D., Stonor, R. W. P., and Moxham, K. E. (1992). "Tests of long plates under biaxial compression." *J. Construct. Steel Res.* 25-56.

Bradford, M. A., Smith, S. T., and Oehlers, D. J. (2000). "Semi-compact steel plates with unilateral restraint subjected to bending, compression and shear." *J. Construct. Steel Res.* 56, 47-67.

Bridge, R. Q., O'Shea, M. D., Gardner, P., Grigson, R., Tyrell, J. (1995). "Local buckling of square thin-walled steel tubes with concrete infill." *Proc. Int. Conf. Struct. Stability & Design*, Sydney, Australia, 307-314.

Bulson, P. S. (1970). *The Stability of Flat Plates*. Chatto and Windus, London.

Davidson, P. C., Chapman, J. C., Smith, C. S., and Dowling, P. J. (1989). "The design of plate panels subject to in-plane shear and biaxial compression." *Royal Int. Nav. Arch.* 267-280.

Dier, A. F., and Dowling, P. J. (1984). "The strength of plates subjected to biaxial forces." *Behaviour of Thin Walled Structures* (Rhodes J. and Sperce J., eds), Elsevier Applied Science Publishers, London, 329-353.

Ge, H. B., and Usami, T. (1992). "Strength of concrete-filled thin-walled steel box columns: experiment." *J. Struct. Eng.* 118(11), 3036-3054.

Ge, H. B., and Usami, T. (1994). "Strength analysis of concrete-filled thin-walled box columns." *J. Construct. Steel Res.* 30, 259-281.

Guedes Soares, C., and Gordo, J. M. (1996). "Compressive strength of rectangular plates under biaxial load and lateral pressure." *Thin-Walled Struct.* 24, 231-259.

Liang, Q. Q., and Patrick, M. (2001). *Design of the Shear Connection of Simply-Supported Composite Beams*. Design Booklet DB1.2, Composite Structures Design Manual, OneSteel Manufacturing Pty Limited, Sydney.

Liang, Q. Q., and Uy, B. (1998). "Parametric study on the structural behaviour of steel plates in concrete-filled fabricated thin-walled box columns." *Adv. Struct. Eng.* 2(1), 57-71.

Liang, Q. Q., and Uy, B. (2000). "Theoretical study on the post-local buckling of steel plates in concrete-filled box columns." *Comput. & Struct.* 75(5), 479-490.

Liang, Q. Q., Uy, B., Wright, H. D., and Bradford, M. A. (2003). "Local and post-local buckling of double skin composite panels." *Proc. Inst. Civ. Eng. Struct. & Builds.* 156(2), 111-119.

Little, G. H. (1977). "Rapid analysis of plate collapse by live-energy minimisation." *Int. J. Mech. Sci.* 19(12), 725-744.

Mendera, Z. K. (1994). "Interaction stability criteria in combined states of stresses for metal plates and shells." *Thin-Walled Struct.* 20, 97-108.

Mofflin, D. S., and Dwight, J. B. (1984). "Buckling of aluminium plates in compression." *Behaviour of Thin Walled Structures* (Rhodes J. and Sperce J., eds), Elsevier Applied Science Publishers, London, 399-427.

Oduyemi, T. O. S., and Wright, H. D. (1989). "An experimental investigation into the behaviour of double–skin sandwich beams." *J. Construct. Steel Res.*, 14, 197-220.

Oehlers, D. J., and Coughlan, C. G. (1986). "The shear stiffness of stud shear connections in composite beams." *J. Construct. Steel Res.* 6, 273-284.

Ollgaard, J. G., Slutter, R. G., and Fisher, J. W. (1971). "Shear strength of stud shear connectors in lightweight and normal-weight concrete." *AISC Eng. J.* 8, 55-64.

Ramberg, W., and Osgood, W. R. (1943). "Description of stress-strain curves by three parameters." *NACA Technical Note*, No. 902.

Roberts, T. M., Edwards, D. N., and Narayanan, R. (1996). "Testing and analysis of steel-concrete-steel sandwich beams." *J. Construct. Steel Res.* 38(3), 257-279.

Shanmugam, N. E., Kumar, Ghanshyam, and Thevendran, V. (2002). "Finite element modelling of double skin composite slabs." *Finite Elements Ana. Des.* 38, 579-599.

STRAND7. G + D Computing Pty Ltd, Sydney, 2000.

Tomlinson, M., Chapman, M., Wright, H. D., Tomlinson, A., and Jefferson A. (1989). "Shell composite construction for shallow draft immersed tube tunnels." *ICE Int. Conf. on Immersed Tube Tunnel Techniques,* Manchester, UK.

Ueda, Y., Rashed, S. M. H., and Paik, J. K. (1995). "Buckling and ultimate strength interaction in plates and stiffened panels under combined inplane biaxial and shear forces." *Marine Struct.* 8, 1-36.

Uy, B. (2000). "Strength of concrete-filled steel box columns incorporating local buckling." *J. Struct. Eng.* 126(3), 341-352.

Uy, B., and Bradford, M. A. (1995). "Local buckling of thin steel plates in composite construction: experimental and theoretical study." *Proc. Instn Civ. Eng. Struct. & Builds,* 110, 426-440.

Uy, B., Wright, H. D., and Bradford, M. A. (2001). "Combined axial and flexural strength of profiled composite walls." *Proc. Instn Civ. Eng. Struct. & Builds,* 146(2), 129-139.

Valsgard, S. (1980). "Numerical design prediction of the capacity of plates in biaxial in-plane compression." *Comput. & Struct.* 12, 729-739.

Williams, D. G., and Walker, A. C. (1975). "Explicit solutions for the design of initially deformed plates subject to compression." *Proc. Instn Civ. Eng.* Part 2, 59, 763-787.

Wright, H. D. (1993). "Buckling of plates in contact with a rigid medium." *The Struct. Eng.* 71(12), 209-215.

Wright, H. D. (1995). "Local stability of filled and encased steel sections." *J. Struct. Eng.* 121(10), 1382-1388.

Wright, H. D., and Oduyemi, T. O. S. (1991). "Partial interaction analysis of double skin composite beams." *J. Construct. Steel Res.*, 19(4), 253-283.

Wright, H. D., Oduyemi, T. O. S., and Evans, H. R. (1991a). "The experimental behaviour of double skin composite elements." *J. Construct. Steel Res.*, 19(2), 97-110.

Wright, H. D., Oduyemi, T. O. S., and Evans, H. R. (1991b). “The design of double skin composite elements.” *J. Construct. Steel Res.*, 19(2), 111-132.

Figures and Tables

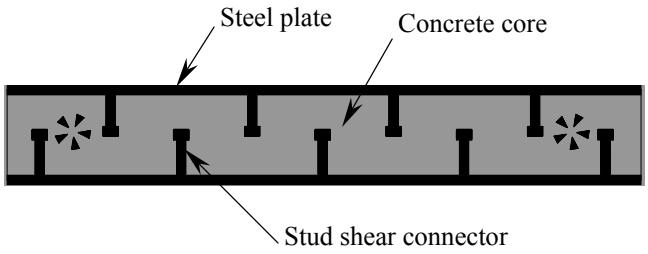

Fig. 1. Cross-section of double skin composite panel

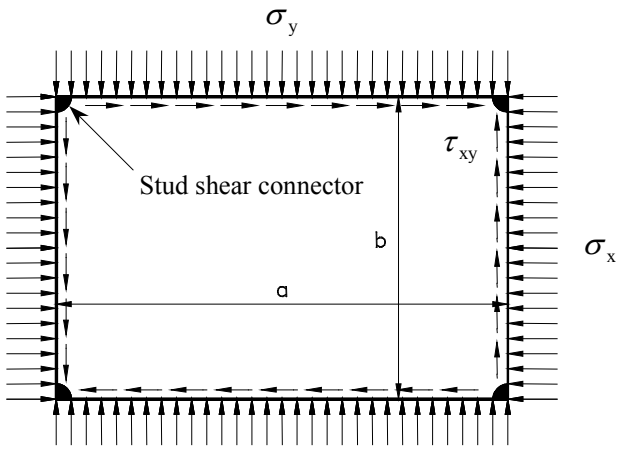

Fig. 2. Single plate field restrained by stud shear connectors

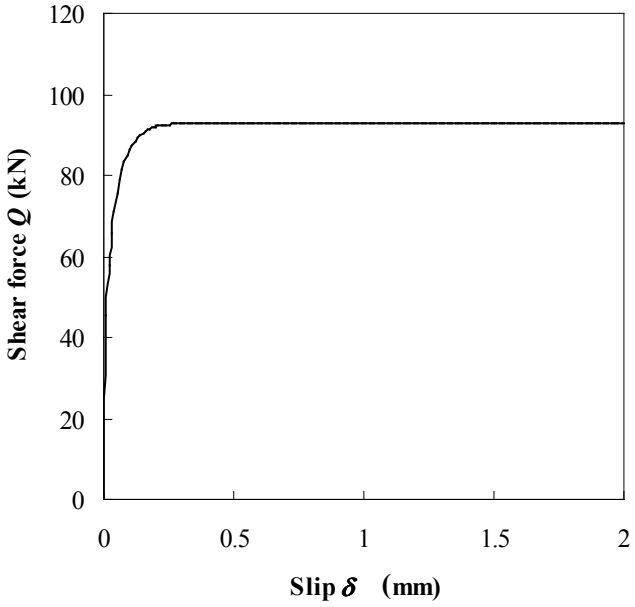

Fig. 3. Shear-slip curve for stud shear connectors

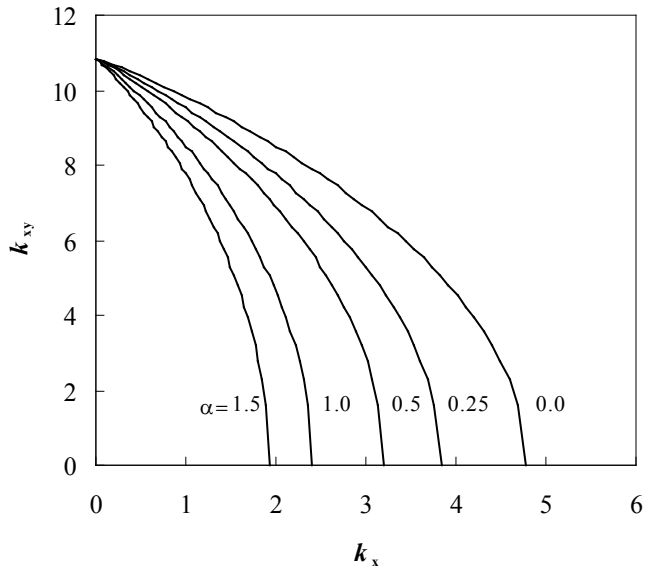

Fig. 4. Buckling interaction curves of plates (S-S-S-S+SC)

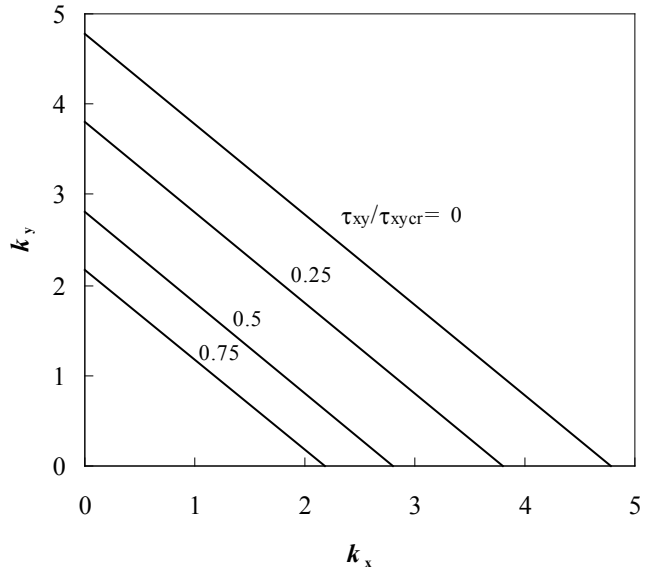

Fig. 5. Buckling interaction curves of plates under constant shear stresses (S-S-S-S+SC)

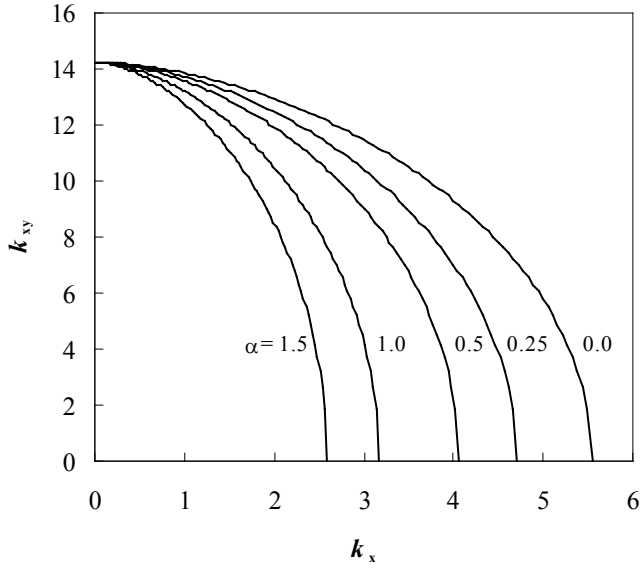

Fig. 6. Buckling interaction curves of plates (C-S-S-S+SC)

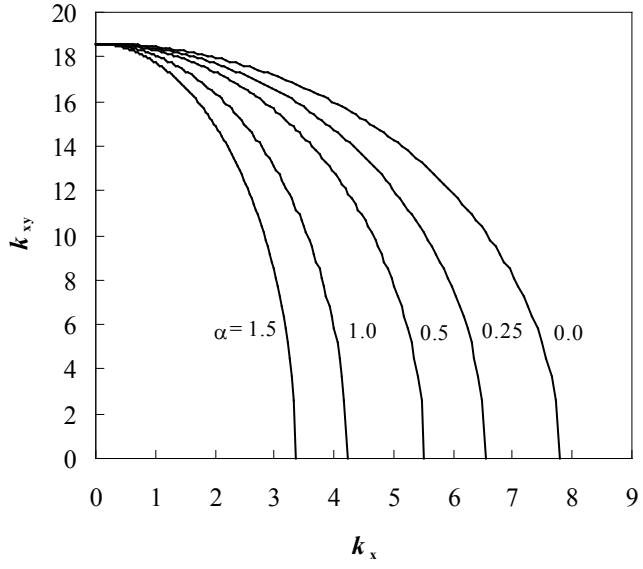

Fig. 7. Buckling interaction curves of plates (C-C-S-S+SC)

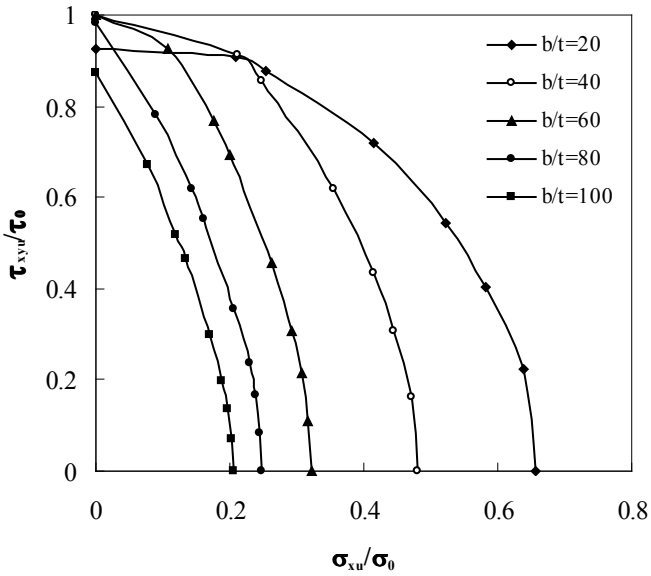

Fig. 8. Strength interaction curves of plates with various *b/t* ratios

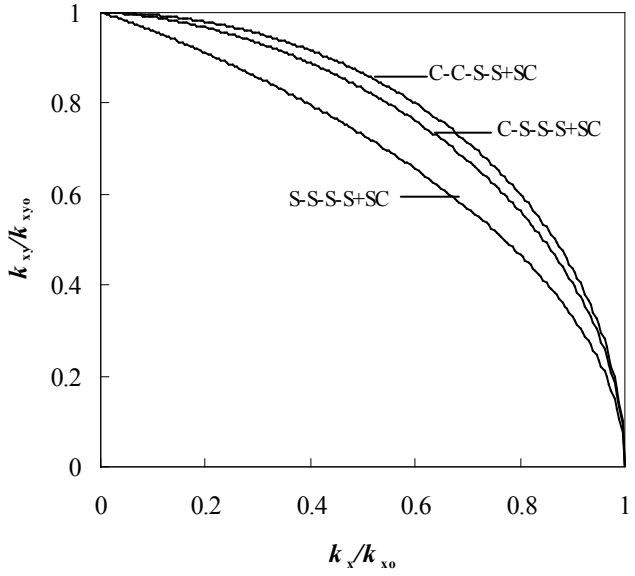

Fig. 9. Normalized buckling interaction curves of plates with different boundary conditions

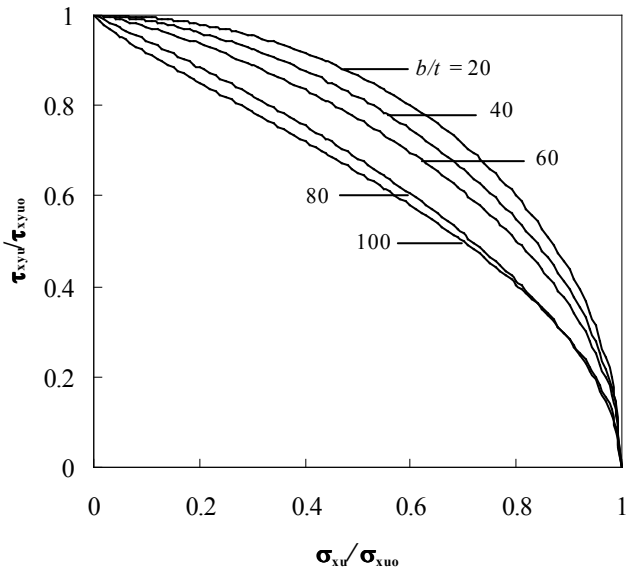

Fig. 10. Strength interaction curves of plates by proposed design models

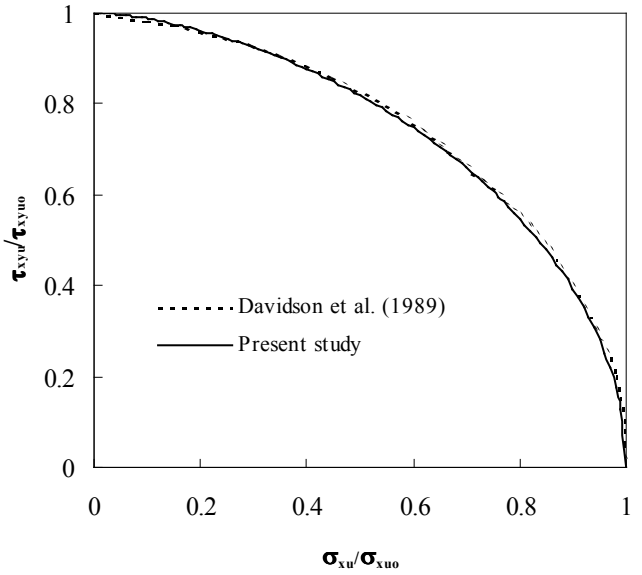

Fig. 11. Comparison of present study with existing results for plate with *b/ t*= 40

Table 1. Parameters for Buckling Interaction Models

Boundary condition (1)	k_{xo} (2)					k_{xyo} (3)	ξ (4)
	α=0	α=0.25	α=0.5	α=1.0	α=1.5		
S-S-S-S+SC	4.782	3.84	3.204	2.404	1.923	10.838	1.1
C-S-S-S+SC	5.552	4.705	4.06	3.168	2.589	14.249	1.7
C-C-S-S+SC	7.797	6.56	5.514	4.216	3.362	18.596	2

Table 2. Parameters for Strength Interaction Models

b/t (1)	σ_{xuo}/σ_0 (2)	τ_{xyuo}/τ_0 (3)	ζ (4)
20	0.658	0.927	2
40	0.481	1	1.6
60	0.321	1	1.3
80	0.248	0.984	1.1
100	0.205	0.875	0.8